EEET ECOLOGICAL ENGINEERING
& ENVIRONMENTAL TECHNOLOGY

Ecological Engineering & Environmental Technology 2021, 22(4), 53–65
https://doi.org/10.12912/27197050/137868
ISSN 2719-7050, License CC-BY 4.0

Received: 2021.04.22
Accepted: 2021.05.15
Published: 2021.06.07

Investigation of the Process of Mud Filtrate Invasion from an Open Wellbore into a Fresh Water Formation

Oleg M. Mandryk[1], Bohdan Mishchuk[1], Andrii I. Zelmanovych[1], Volodymyr V. Tyrlych[1], Oleg M. Tuts[1], Liubov Poberezhna[1*]

[1] Ivano-Frankivsk National Technical University of Oil and Gas, Ukraine
* Corresponding author's email: dlya2906@gmail.com

ABSTRACT
While developing hydrocarbon (oil and gas) deposits, it is necessary to drill into shallow formations of fresh (drinking) water, and this causes the filtrate invasion from the open wellbore into these formations. A mathematical model of this process was created; an analysis of the influence of the identified by the process features filtration zones was performed, and it was shown that the zones of the mud crust and interstitial colmatation are dominant. The filtrate invasion can significantly impair the quality of fresh water and cause environmental damage.

Keywords: ecology of fresh water deposits, fluid filtration, well drilling, oil and gas production.

INTRODUCTION

Ukraine, like many European countries, begins to feel a lack of fresh water from surface water sources or subsurface formations due to their contamination, which leads to active development of the underground aquifers. Three hydrodynamic zones are distinguished within the studied part of the water-bearing formations: free (active) water exchange, impeded water exchange and stagnant regime (Chi, 2011, Gleeson, 2012). The following types of water occur in the first zone up to a depth of about 500 m: fresh or low salinity water, as well as infiltration water and water of various genetic types with the hydrostatic nature of the energy potential (suspended, ground, interformation nonartesian and formation artesian waters). In the second zone, at depths of 500–1500 m, there are formations of artesian waters of chloride-calcium, sometimes chloride-magnesium and hydrocarbon-sodium types with mineralization of 5–10 g/l and hydrostatic nature of energy potential (Tikhomirov, 2018). Below, at depths of 1500–4000 m, in the stagnation zone, there are mainly artesian waters with high mineralization (dozens – the first hundreds of grams per liter) of chloride-calcium type, whose pressures are determined by geostatic pressure, as well as by exfiltration and sedimentation origin (entrapped water), and the role of drainage, rejuvenated and lithogenic waters is increasing with the depth, which determines the hydrogeological inversion (decrease) of mineralization (Adamenko, 2017, Shokri-Kuehni, 2017). At the present time, the underground waters of the first two zones, up to a depth of 1500 m, can be economically feasible for domestic fresh water supply. Underground fresh waters can be found practically on all territory of Ukraine.

This country also has an urgent problem of fuel and energy independence, own-produced oil and gas supply (Misch, 2016). Oil and gas production is connected with three petroliferous areas: Carpathian, Dnipro-Donetsk and Black Sea-Crimean (Sephton, 2013, Misch, 2016,). Oil and gas deposits, which are developed or going to be developed, are mostly located at great depths (Sephton, 2013, Maievskyi, 2014). Thus, when developing hydrocarbon deposits, the surface of fresh and mineral waters has to be drilled, which is one of the factors of negative influence on the quality of fresh water (WHO, 2016, Boiko, 2017, Mandryk, 2017). Consequently, the problem of protecting underground fresh water against contamination during oil and gas production is topical. In order to explore and develop hydrocarbon (oil and gas) deposits, wells (exploration, development, production and injection) are drilled in the upper rock formations, among which there are formations saturated with underground fresh water. To cement the upper unstable intervals of the geological section and isolate the water-bearing formations from contamination, they are blocked by surface casing cemented along the entire length (Reddy, 2012).

If the surface casing is open during drilling (neither cased nor cemented), the wellbore interacts with the invaded water formation hydrodynamically. In accordance with the drilling technology, some excess pressure of the drilling mud in the well is maintained at the level over the possible formation pressure in the water formation (pressure repression). As a result of this pressure repression, the filtrate invasion of the drilling mud into the water formation occurs, the crust of solid phase of the drilling mud (usually the clay crust) is formed, solid phase leads to interporous colmatation, and the filtrate is mixed with the formation water, causing it to become contaminated both by process water, which is used to produce drilling mud, and chemical agents, which are added to the solution to adjust its properties. It should be pointed out that it is forbidden to use chemical agents of hazard Class I and II (for example, sodium hydroxide, sodium aluminate, construction lime) for treatment of drilling muds in the intervals containing fresh water, and during drilling in fresh water intervals, the absorption of drilling fluids and materials should not be allowed in volumes that change the quality and composition of underground waters beyond the established standards (AMSE, 2011).

Taking into account the purpose of the surface casing in the design of oil well, it can be assumed that drilling in order to run this string may be similar to the construction of hydrogeological and water supply wells. Rotary drilling with its normal and reverse circulation prevails and amounts to more than 80% of the total volume of works (Mysliuk, 2002, Veil, 2002) in the practices of drilling for water. The rest includes such types of drilling as cable-tool and auger drilling, as well as drilling using hydraulic core lifter, compressed air drilling, etc. When carrying out rotary drilling, it is recommended to use process water and water-hygienic solutions for circulation within the unstable water-bearing sand formation, and the density of the solution is feasible to be regulated by adding a sodium chloride (Mysliuk, 2002). In other cases, carbonate, chalk, polymeric (based on modified starch with/without bentonite) and bentonite solutions with the special polymeric preparations are used. In this case, preliminary drilling of the exploration well is planned for the purpose of the stratigraphic depth exploration. It should be pointed out that such wells are developed by influx until complete water purification.

In relation to the degree of stability of the well walls during drilling in, development and processing of water-bearing formation, three of its main types (A, B, C) with three subtypes according to the degree of permeability (I, II, III) were distinguished (Mysliuk, 2002). The first type includes inequigranular sand, the second type includes sandstones, siltstones, argillites, limestones and dolomites (fractured and cavernous), and the third type includes dense sandstones, limestones, shales, quartzites, gneisses, granites, porphyrites, and fractured syenites (with capillary and large cracks, as well as faulted zones and cavities). It was found out after industrial researches and observations that in order to ensure the stability of the well walls in the water-bearing sand formation, excess hydrostatic pressure should be 0.03–0.04 MPa above the formation pressure, and later after experiments on a special installation, this excess pressure was confirmed and it was shown that a general collapse of the pit-bottom rocks could occur inside the well in addition to sloughing. It was pointed out that the mechanical colmatation of rocks contributes to the increase in the well wall stability when the formation is drilled in with water circulation (Mysliuk, 2002). This experience is recommended to be used when drilling for the surface casing of the oil well.

The literature on hydrogeology proposes that one of the main sources of underground water contamination is wells of various purposes (Veil, 2002, Bakke, 2013, Mandryk, 2017, Pietrzak, 2018, Chudyk, 2019). The problem of hydrodynamic coupling of an open bore hole and water formation is not highlighted in the known literature. The problems of invasion of mud filtrate, as well as the filtrate and disperse phase, into the oil formation were considered in the literature (Mandryk, 2017), but transferring the results to the water formation is considered as incorrect, since the mutual fluids displacement in the oil formation is described with phase invasions in the presence of capillary pressure. Somewhat closer are the researches on oil displacement with solvents in the technology of oil deposit development (Thomas, 2008) and displacement of fresh waters by saline waters in hydrogeology (Reilly, 1985, Barlow, 2003, Huang, 2009), but they refer only to one displacement zone. The unresolved question of the overall problem of protecting fresh groundwater against contamination during the carbohydrate deposits development concerns the research of hydrodynamic coupling of the open drilled bore hole with the drinking water formation.

The purpose of the work consists in hydrodynamic description of the process of mud filtrate flow into the fresh water-bearing formation from an open bore hole, estimation of the influence of the clay crust and zone of intraporous fluctuation on the process and estimation of the amount of filtrate in the formation.

METHODOLOGY OF RESEARCH

For research, methods of underground hydrogasmechanics, groundwater dynamics and experimental data are used. Given that the filtration tasks with moving limits are extremely complex in the context of movement of liquids and gases in porous and cracked environments, which makes it impossible to obtain the final analytical solution, then we use a method of successive change in stationary states (SCSS) (Christiansen, 1973) which is based on three assumptions:

1) Layer is divided into a finite area of the perturbed movement and the region of an unbreakable state;
2) Within the perturbed region, a pressure distribution law that increases from the pressure of p_c (or pressure of $p_к$) to pressure $p_к$; In an unbreakable region, the pressure everywhere is constant and equal to the pressure $p_к$;
3) The size of the pressure perturbation is determined from additional conditions in relation to a flat-radial stream in the form:

$$R(t) = \sqrt{c_1 \kappa t} \quad (1)$$

or in relation to a straight-parallel stream

$$l(t) = \sqrt{c_2 \kappa t} \quad (2)$$

where: c_1, c_2 – some constant values of integration, which we find based on the initial and marginal conditions for pressure when a constant depression of pressure) or when a permanent debit of gallery;

R(t) and *l(t)* – radius and length, respectively, the distribution zone of pressure depression measles at time *t* after the well start.

It should be noted that in the real conditions of perturbation in the reservoir extends with the speed of sound. But if, based on the law of Darcy and neglecting inertial forces, we received a piezoconductivity equation to add here $\kappa = k/\mu\beta$, then the rate of distribution of perturbations in general in this case is boundless, that is, in such an idealized pressure perturbation scheme immediately (instantaneously) extends all over layer. In fact, the amplitude of the perturbation of pressure in the reservoir on the wave front due to the occurrence of filtration friction fades approximately exponent to a distance passed by a wave. According to the SCSS, the distribution of pressure in the perturbed zone of the reservoir is given by a straight line (rectilinear-parallel flow) or a logarithmic curve (flat-radial flow), that is, as in the case of established filtration (Fig. 1):

$$p(x,t) = p_к - \frac{Q\mu}{kF}\left[l(t) - x\right] \quad (3)$$

$$p(r,t) = p_к - \frac{Q\mu}{2\pi kh}\ln\frac{R(t)}{r} \quad (4)$$

where: LCD – permanent initial pressure in the reservoir; Q – debit; μ – coefficient of dynamic viscosity; k – coefficient of permeability; h – thickness of the formation

Relative calculations errors in comparison with precise formulas do not exceed 11–25% for the flow to the gallery (11% for Δp_0 = const and 25% per) and 6–15% (10–15% for Δp_0 = const and 6% for Q_0 = const) for the drill. Such a large error is due to a significant distortion of the actual pressure distribution curve in the reservoir.

RESULTS AND DISCUSSION

The interaction of the open wellbore and endless water formation with the mud filtrate invasion from the well under the action of pressure repression as a function of time with a variable boundary of the displacement zone. Four zones can be distinguished: clay crust; intraporous colmatation; displacement of formation water by filtrate; unsteady filtration of formation water. Each zone was characterized by geometric dimensions and invasions that are variable in time. The tasks of filtration with moving boundaries are

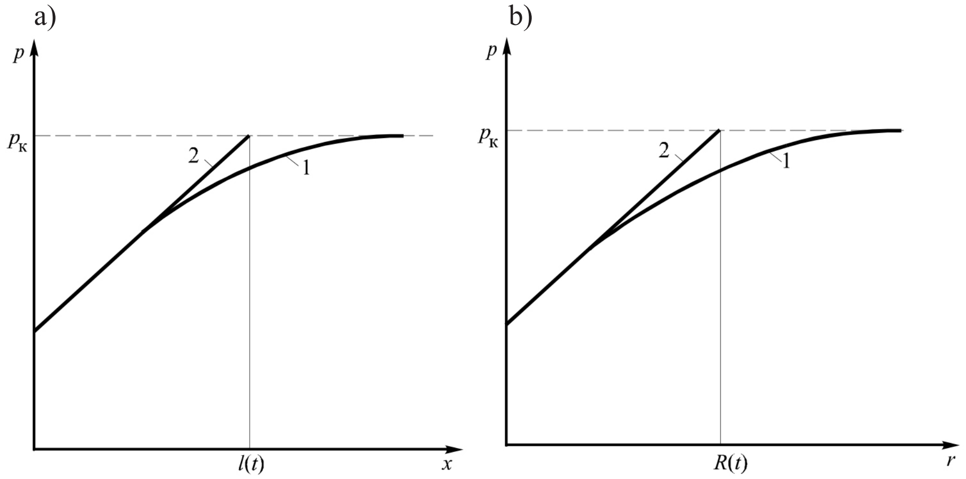

Figure 1. Distribution of pressure in the reservoir on elastic mode (1) in relation to rectilinear-parallel (a) and flat-radial (b) streams and its interpretation (2) by the method of successive change of stationary states

extremely complicated in underground hydrogasmechanics, which makes impossible to obtain the final analytical solution, so in our case the method of sequential change of stationary states was used (Christiansen, 1973).

When assuming that the filtrate is incompressible (it is quite possible in case of small pressure changes) and associating the filtrate flow with the displacement boundary position, the constant flow rate $Q(t)$ at a certain time t in different zones can be calculated. The size of the zones, the conductivity of which is different, changes in time, therefore, in the process of the considered interaction, there is a change in the filtration resistance and fluid flow rate in the formation (the pressure in the well is maintained constant from the standpoint of the drilling technology).

Furthermore, the liquid Q flow amounts to (Misch, 2016) according to the linear Darcy law for each zone (in our case, the violation of the linear law is unlikely to happen) (Mysliuk, 2002):

$$Q = \frac{k}{\mu}\frac{dp}{dr}2\pi hr \qquad (5)$$

or

$$dp = \frac{Q\mu}{2\pi h}\frac{dr}{kr} \qquad (6)$$

where: k – coefficient of the medium permiability; μ – dynamic coefficient of liquid viscosity; p – pressure; h – medium thickness (vertically); r – movable radius.

Clay crust zone. After integrating the equation (2), a loss of pressure in this zone is calculated:

$$\Delta p_{г}(t) = \frac{Q(t)\mu_{ф}}{2\pi h}\int_{r_{г}(t)}^{r_{c}}\frac{dr}{k_{г}(t)r} \qquad (7)$$

where: $\mu_{ф}$ – dynamic coefficient of viscosity of the clay mud filtrate; $r_{Г}(t)$ – internal radius of clay crust as a function of time t; r_{c} – well radius along the drill bit; $k_{Г}(t)$ – coefficient of permeability of clay cake as a function of time t.

The filtrate invasion into the formation occurs through the clay crust, which is formed as a microporous structure of increasing thickness (in radius) and further determines the solid phase flow in the rock structure pores of the water-bearing formation and intensity of the filtrate invasion into the formation. The decline of the invasion process essentially depends on the type of mud and occurs during 100–300 h, i.e. the coefficient of crust permeability significantly decreases. Formation of clay crust and zone of colmatation occurs simultaneously and almost ends in 20–40 min (Boiko, 2014). Under the dynamic conditions, the thickness of the crust is stabilized after the surface ablation with the flow of clay solution and it is approximately the same and is within 5–15 mm in formation with substantially different reservoir properties (Boiko, 2014). The coefficient of the clay crust permeability decreases to 10^{-19}–10^{-15} m^2 and depends on the clay properties, content of sand, mechanical impurities (sludge) and chemical agents in the solution, as well as on the drop of pressure (Boiko, 2014).

The speed of filtration is determined by the filtration resistance of the rock, filtration processes, crust formation and colmatation. Clay solutions, including solutions weighted with barite, with the finely dispersed phase are filtered with lower velocity of filtration decline than solutions with optimal content of large particles in the disperse phase. The initial velocity of filtration of clay solutions that are not weighted and are weighed with barite is greater than that of the solutions with an adhesionally inactive solid phase. If the filtration of chalk solutions practically ceases within 3–5 days, the filtration of clay and weighed clay solutions continues for a longer period of time (Caenn, 1996, Mitchell, 2006).

Taking into account the above mentioned and based on the experimental data (Boiko, 2014), the temporal variation in the clay crust thickness is described by the exponential law:

$$h_\Gamma(t) = h_\Gamma\left(1 - e^{-a_1 t}\right) \tag{8}$$

and the coefficient of permeability is calculated in the same way:

$$k_\Gamma(t) = k_\Gamma e^{-a_2 t^{a_3}} \tag{9}$$

where: h_Γ – stable thickness of the crust, m; t – time, s; k_Γ – coefficient of crust permeability according to the laboratory data at the initial moment of its formation, m^2; a_1, a_2 – empirical coefficients. Here, h_Γ= (5–15)·10^{-3} m, $k_\Gamma = k$; k – coefficient of rocks permeability, m^2. Change of relative thickness $\bar{h}_\Gamma(t) = h_\Gamma(t)/h_\Gamma$ and relative permeability coefficient $\bar{k}_\Gamma(t) = k_\Gamma(t)/k_\Gamma$ depending on time t is shown on Figure 2.

From that follows that during 30 days filter-cake thickness gets closer to its highest value when coefficient a_1 is within from 0.0000025 to 0.0001and permeability decreases practically to zero at coefficient a_2 values within from 0.27 to 0.9 and a_3 – from 0.1 to 0.22. Coefficients a_1, a_2, and a_3 define process of cake formation which depends on drilling mud type and porous characteristics of rock formation permeability (those are subject to an experimental definition in specific conditions).

Then the drop of pressure, depending on the time t in the clay crust zone, is calculated in the following way:

$$\Delta p_\Gamma(t) = \frac{Q(t)\mu_\phi}{2\pi hk}\frac{1}{e^{-a_2 t^{a_3}}}\ln\frac{r_c}{r_c - h_\Gamma(1-\exp(-a_1 t))} \tag{10}$$

where: $r_\Gamma(t) = r_c - h_\Gamma(t) = r_c - h_\Gamma(1 - e^{-a_1 t})$.

Zone of intraporous colmatation. It is formed as a result of the flow of solid and colloidal particles of clay solution with the filtrate into the formation. The formation of the colmatation zone (thickness) and (permeability) in time is described in the same way as the formation of the clay crust zone, namely:

$$h_k(t) = h_k(1 - e^{-a_4 t}) \tag{11}$$

$$k_k(t) = k_k e^{-a_5 t^{a_6}} \tag{12}$$

where: h_k – formed wall packing (colmatation) zone thickness (in radius); k_k – coefficient of permeability in wall packing zone at initial moment and equals

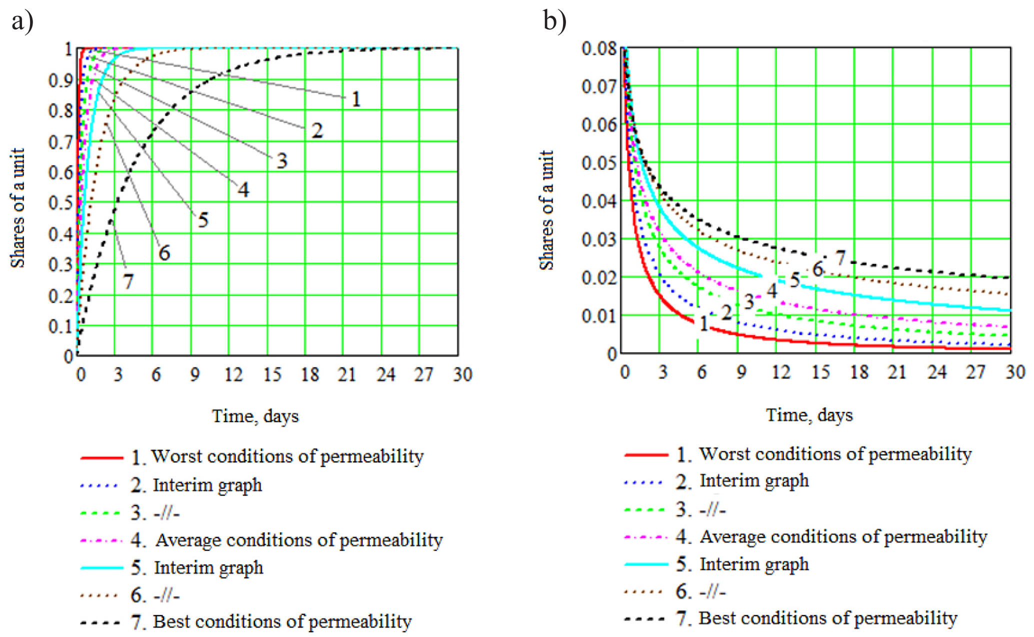

Figure 2. Change of relative wall cake thickness (a) at a_1, s^{-1} equals 1 – 0.0001; 2 – 0.000048; 3 – 0.00003; 4 – 0.0000205; 5 – 0.000013; 6 – 0.000007; 7 – 0.0000025 and change of relative permeability coefficient of wall cake (b) at a_2, s^{-1} equals 1 – 0.27; 2 – 0.32; 3 – 0.38; 4 – 0.47; 5 – 0.57; 6 – 0.71; 7 – 0.9 and a_3 equals 1 – 0.22; 2 – 0.2; 3 – 0.18; 4 – 0.16; 5 – 0.14; 6 – 0.12; 7 – 0.1.

to coefficient of permeability of water layer rock;

$k_к = k$ (before wall packing zone was forming);

a_4, a_5, a_6 – empirical coefficients.

Invasion of the mud solid (dispersed) phase (free-bound disperse system) occurs in porous and fissured formations, which are bound dispersed system, i.e. colmatation may occur, and the channels diameters and solution particles diameters, for example, random values, are subject to certain laws of statistical distribution (Ghassal, 2019). Since the statistical distribution of the particles diameters (sizes) was not investigated (and it is not the subject of this research), the research will be restricted to the known laboratory analyses on formation of the colmatation zone (Ghassal, 2019). The depth of the colmatation zone is determined by the porous characteristic of the porous medium and multidimensional particles of the fine-dispersed phase of the solution, it does not exceed 12–16 mm in the porous and small cavernous reservoirs (Ghassal, 2019), and the particles in the pores are arranged chaotically, their placing is loose and inhomogeneous (Goldberg, 1976).

Thus, at $h_к = (10–15)\cdot 10^{-3}$ m and t = 1200–2400 s, coefficient $a_4 = 0.00045$ c^{-1}, and at $\overline{k}_к(t) = k_к(t)/k = 10^{-5}–10^{-2}$ and t = 1200–2400 s coefficients $a_5 = 2\cdot 10^{-7}$ c^{-1} and $a_6 = 7\cdot 10^{-6}$ c^{-1}. Under conditions described above these coefficients reach different values and must to be defined in an experimental research. The time change of $\overline{h}_к(t) = h_к(t)/h$ and $\overline{k}_к(t) = k_к(t)/k$ depending on time t is shown in Figure 3.

Similar conclusions can be made based on Figure 2 regarding the formation of the zone of intraporous colmatation, so the thickness (along the radius) of the clay crust and zone of intraporous colmatation increases in time, and, accordingly, the coefficients of permeability decrease according to experimental data.

Thus, for the zone of intraporous colmatation, the value of the pressure drop can be calculated with regard to time value t:

$$\Delta p_к(t) = \frac{Q(t)\mu_ф}{2\pi hk}\frac{1}{e^{-a_5 t^{a_6}}}\ln\frac{r_c + h_к(1-\exp(-a_4 t))}{r_c} \quad (13)$$

where: $r_к(t) = r_c - h_к(t) = r_c - h_к(1 - e^{-a_4 t})$ – external radius of the colmatation zone.

Zone of fresh water displacement by filtrate. Mud filtrate displaces fresh water in the displacement zone. To drill a large diameter wellbore, 60–80 kg of bentonite and 1 kg of caustic soda (sodium hydroxide NaOH) are added into 1 m^3 of fresh (technical) water (Sephton, 2013). The density of this solution is 1150 kg/m^3, the viscosity of the taper bar is 100–120 s, pH = 10–11, and the filtration rate is usually not controlled. 50 kg of bentonite, 2 kg of caustic soda and 15–20 kg of high-viscosity carboxyl methylcellulose (CMC) shall be added to 1 m^3 of sea or salt water (50 kg of sodium chloride NaCl per 1 m^3 of fresh water). 50 kg of bentonite, 2 kg of caustic soda and 15–20 kg of high-viscosity carboxyl methylcellulose

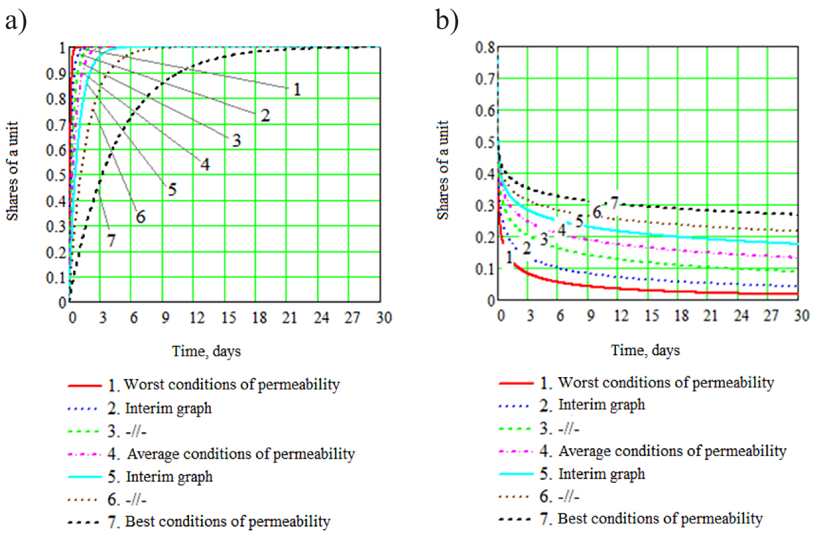

Figure 3. Change of relative thickness (a) of intra-porous wall packing zone when a_4, s^{-1} equals 1 – 0.0001; 2 – 0.000048; 3 – 0.00003; 4 – 0.0000205; 5 – 0.000013; 6 – 0.000007; 7 – 0.0000025, and relative coefficients of permeability (b) of intra-porous wall packing zone when a_5, s^{-1}, equals 1 – 0.16; 2 – 0,165; 3 – 0.17; 4 – 0.19; 5 – 0.22; 6 – 0.26; 7 – 0.3 and a_6 equals 1 – 0.22; 2 – 0.2; 3 – 0.18; 4 – 0.16; 5 – 0.14; 6 – 0.12; 7 – 0.1.

(CMC) shall be added to 1 m^3 of sea or salt water (50 kg of sodium chloride NaCl per 1 m^3 of fresh water). It should be noted that NaOH belongs to Class II of hazard (high hazardous), NaCl, CMC, Na_2CO_3 – to Class III (moderately hazardous), and bentonite powder – to Class IV (low hazardous) (Misch, 2016). Consequently, fresh water in the formation is displaced from the well by technical water with impurities of chemical agents of different hazard classes. If the viscosity and water density are equal to 1 m Pa·s and 1000 kg/m^3 with the salinity of 1g/l and the temperature of 20 °C, mineralization of 40 g/l (mineralization of saline ground water rarely exceeds 50 g/l and is usually 5–15 g/l) is respectively 1.04 m Pa·s and 1020 kg/m^3. Thus, the system of mud filtrate and underground water with mineralization of 1–15 g/l can be considered homogeneous and the difference in permeability for fresh and salty waters (taking into account different level of shale hydration) will be negligible and can be neglected.

There are two models of displacement in hydromechanics of mutual fluid displacement: a) piston-like displacement, when there is a clear boundary between the displacement and displaced fluids, in front of which only the displaced fluid moves, and behind of which only the displacement fluid moves; b) non-piston-like displacement, in which displacement and displaced fluids are simultaneously moving in the displacement zone (Thomas, 2008). The second scheme includes two or three single phases (for example, water and oil phases) with possible change in phase, and it is based on the concepts of phase permeability and takes into account hydrodynamic, gravitational and capillary forces. According to the first scheme, the liquid (phases) can have only one type (fresh and saline water), there is no capillary pressure and liquids mix without limits, as well as differ in particular mineralization, density and viscosity.

In the water-rock system, processes of sorption, ion exchange, dissolution, hydration, and hydrolysis can actively occur; the composition and quantity of substances in water are continuously mixing, so that the water filtration process is complicated by the transfer of substances. Transfer of substances occurs by convective (or filtration) water flow and conductive (or diffusion) flow in still water molecularly (Boiko, 2017). There is an intense mixing of the solution during the movement of the water solution in a heterogeneous (porous or crumbling) structure due to fluctuation of the values and directions of local true velocities in a complicated pore system (chaotically oriented in space, variable cross section and irregular shape, with different roughness of the walls surface), crumbles and macro heterogeneity (lithological-and-granulometric, packaging, mineral, cementation, porous, penetrating, volume-and-thickness, areal) (Mysliuk, 2002) and this transfer mechanism with the imposition of molecular diffusion is called convective filtration diffusion or hydrodynamic dispersion (hydrodispersion). The diffusion occurs under the influence of gradients of concentration, temperature, pressure, as well as electric, magnetic and gravitational fields. The analysis of these phenomena has shown (Barlow, 2003, Thomas, 2008, Huang, 2009) that the named processes (sorption, dissolution, etc.) and diffusion transitions (formation of the "finger" of the heavy liquid at the formation bottom, "blurring" of distinction between fresh and saline waters, etc.) can be ignored, and the scheme of the piston displacement can be used for practical calculations of the change in the water displacement front (Reilly, 1985, Barlow, 2003, Thomas, 2008, Huang, 2009).

The influence of the flow hydrodispersion is taken into account in the coefficients of permeability for the filtrate:

$$k_{\text{в}}(t) = ke^{-a_7 t^{a_8}} \tag{14}$$

and coefficients of porosity in the displacement zone:

$$m_{\text{в}} = a_9 m(1 - s_{\text{п.в.}}) \tag{15}$$

where: k – coefficient of water formation permeability; a_7, a_8, a_9 – empirical coefficients; m – coefficient of porosity of the water formation; $s_{\text{п.в.}}$ – saturation of pores by bound and irreducible water.

Here, m is the coefficient of active rock porosity, which is the ratio of the filtration pore volume with water and open to filtration of filtrate and total pore volume of the rock sample. The change $\bar{k}_{\text{В}}(t) = k_{\text{В}}(t)/k$ depending on time t is shown in Figure 4.

Then, for the displacement zone, the drop of pressure, depending on the time t will be indicated

$$\Delta p_{\text{в}}(t) = \frac{Q(t)\mu_{\phi}}{2\pi kh} \frac{1}{e^{-a_7 t^{a_8}}} \ln \frac{r_{\text{в}}(t)}{r_{\text{c}} + h_{\text{к}}(1 - \exp(-a_4 t))} \tag{16}$$

where: $r_{\text{В}}(t)$ – external radius of the displacement zone, which is unknown and subject to evaluation.

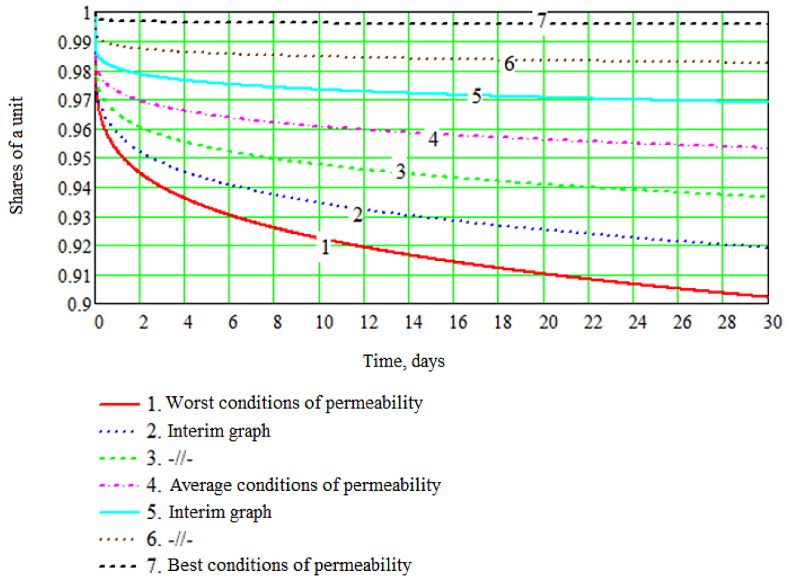

Figure 4. Change of relative permeability coefficient in mud-water displacement zone over time when coefficient a_7, s^{-1}: 1 – 0.004; 2 – 0.0044; 3 – 0.0046; 4 – 0.0045; 5 – 0.004; 6 – 0.003; 7 – 0.001; a_8: 1 – 0.22; 2 – 0.2; 3 – 0.18; 4 – 0.16; 5 – 0.14; 6 – 0.12; 7 – 0.1; in all cases a_9 equals 0.85.

The position of the displacement zone boundary, i. e. the radius $r_{â}(t)$, will be connected with time through the equation of the material balance

$$\int_0^t Q(t)dt = \pi h(m_г(r_c^2 - r_г^2) + m_к(r_к^2 - r_c^2) + m_в(r_в^2(t) - r_к^2)) \quad (17)$$

or at $r_k \approx r_c \approx r_T$ (since $r_k - r_c \leq 50$ mm, $r_c^2 - r_T^2 \leq$ 15 mm):

$$\int_0^t Q(t)dt \cong \pi h m_в (r_в^2(t) - (r_c + h_к(1 - e^{-a_3 t}))^2) \quad (18)$$

where: m_T, m_k – coefficients of porosity, correspondingly, in the zones of both crust and colmatation; h – thickness of the water-bearing formation.

Zone of unstable filtration of formation water. The perturbation of pressure, elastic compression of water and rock occurs during the filtrate flow into the water formation in the water zone. The water formation is assumed to be infinite; the pressure repression and fluid flow are variable in time, and then the zone radius of the pressure perturbation can be calculated with the formula (Goldberg, 1976):

$$r_{зб}(t) = r_c + \sqrt{2.66\kappa t} \approx \sqrt{2,66\kappa t} \quad (19)$$

where: $\kappa = k/\mu\beta^*$ – coefficient of piezoconductivity of the water formation in its original state; μ – dynamic coefficient of viscosity of formation water; $\beta^* = m\beta_B + \beta_c$ – coefficient of elastic capacity of water-saturated formation; β_B – coefficient of volume compression of water or coefficient of volume elasticity of water, for fresh water, $\beta_B = 4.62 \cdot 10^{-10}$ Pa^{-1}; β_c – coefficient of volume elasticity of the formation matrix, $\beta_c = (0.3–2) \cdot 10^{-10}$ Pa^{-1}. Consequently, the drop of pressure in the water zone is written using the method of successive change of stationary states as follows:

$$\Delta p_{в.з.}(t) = \frac{Q(t)\mu}{2\pi k h} \ln \frac{\sqrt{2.66\kappa t}}{r_в(t)} \quad (20)$$

As a result, the total drop of pressure in the water formation is

$$\Delta p = \Delta p_г(t) + \Delta p_к(t) + \Delta p_в(t) + \Delta p_{в.з.}(t) \quad (21)$$

or

$$\Delta p = Q(t)\Omega(t) \quad (22)$$

or

$$Q(t) = \frac{\Delta p}{\Omega(t)} \quad (23)$$

where: Δp – total pressure drop (pressure repression) as the difference between the pressure in the well, which is maintained constant according to the drill technology, and pressure in the water formation at the boundary of the perturbation pressure zone (also constant), and constant pressure repression Δp is maintained at each moment of time t of pressure redistribution between allocated zones; $\Omega(t)$ – total filtration resistance,

$$\Omega(t)=\frac{2\pi kh\Delta p}{\mu_{\text{в}}}\Big(\frac{\bar{\mu}_{\text{ф}}}{e^{-a_2t^{a3}}}\ln\frac{r_{\text{с}}}{r_{\text{с}}-h_{\text{г}}(1-\exp(-a_1t))}+ +\frac{\bar{\mu}_{\text{ф}}}{e^{-a_4t^{a5}}}\ln\frac{r_{\text{с}}+h_{\text{к}}(1-\exp(-a_6t))}{r_{\text{с}}}+ +\frac{\bar{\mu}_{\text{ф}}}{e^{-a_7t^{a_8}}}\ln\frac{r_{\text{в}}(t)}{r_{\text{с}}+h_{\text{к}}(1-\exp(-a_4t))}+\ln\frac{\sqrt{2.66\kappa t}}{r_{\text{в}}(t)}\Big) \quad (24)$$

where: $\bar{k}_{\text{Г}} = k_{\text{Г}}/k$; $\bar{k}_{\text{к}} = k_{\text{к}}/k$; $\bar{\mu}_{\text{Ф}} = \mu_{\text{Ф}}/\mu$.

In this case the filtrate flow $Q(t)$ and radius of the zone of fresh water displacement by mud filtrate $r_{\text{В}}(t)$ are unknown as a function of time t, they are connected with each other by the equation of material balance with the accumulated filtrate flow $Q_{\text{Н}}(t) = \int_0^{t_i} Q(t)dt$. Then the solution is based on a combined solution of equations (14) and (19). To solve this, we must split a studied period of time into equal intervals (for example 30 days) Δt = 0.0347 day (the smaller the interval Δt, the more accurate the result is going to be); the number of intervals equals n = 30/0.0247 = 865. Time is found from the equation: $t_i = t_{i-1} + \Delta t$; when $i = 1$ time is $t_{i-1} = t_0 = 0$, $t_1 = \Delta t$, when $i = 2$ time is $t_2 = t_1 + \Delta t$ etc.

According to accumulated filtrate rate will be defined as limit function of sum of zones:

$$Q_{\text{н}_i} = \int_0^{t_i} Q(t)dt = \sum_0^{t_{i-1}} Q_{i-1}\Delta t + Q_i\Delta t \quad (25)$$

where: Q_{i-1}, Q_i – filtrate flow at appropriate intervals of time; at $i = 1$ the flow is $Q_{i-1} = 0$.

Thus, the expression (14) is rewritten as:

$$\sum_0^{t_{i-1}} Q_{i-1}\Delta t + Q_i\Delta t = \pi hm_{\text{в}}(r_{\text{в}}^2(t_i) - (r_{\text{с}} + h_{\text{к}}(1-e^{-a_4t_i}))^2) \quad (26)$$

whence:

$$Q_i = \frac{1}{\Delta t}(\pi hm_{\text{в}}(r_{\text{в}}^2(t_i) - (r_{\text{с}} + h_{\text{к}}(1-e^{-a_4t_i}))^2) - \sum_0^{t_{i-1}} Q_{i-1}\Delta t) \quad (27)$$

Equate the expressions (19) and (23) and for clarity we will write them in less complicated way in a functional form:

$$M_i(r_{\text{в}}(t_i)) = N_i(r_{\text{в}}(t_i)) \quad (28)$$

where:

$$M_i(r_{\text{в}}(t_i)) = \frac{1}{\Delta t}(\pi hm_{\text{в}}(r_{\text{в}}^2(t_i) - (r_{\text{с}} + h_{\text{к}}(1-e^{-a_4t_i}))^2 - \sum_0^{t_{i-1}} Q_{i-1}\Delta t) \quad (29)$$

$$N_i(r_{\text{в}}(t_i)) = \frac{2\pi kh\Delta p}{\mu}\Big(\frac{\bar{\mu}_{\text{ф}}}{e^{-a_2t^{a3}}}\ln\frac{r_{\text{с}}}{r_{\text{с}}-h_{\text{г}}(1-\exp(-a_1t))}+ + +\frac{\bar{\mu}_{\text{ф}}}{e^{-a_4t^{a5}}}\ln\frac{r_{\text{с}}+h_{\text{к}}(1-\exp(-a_6t))}{r_{\text{с}}}+ +\frac{\bar{\mu}_{\text{ф}}}{e^{-a_7t^{a_8}}}\ln\frac{r_{\text{в}}(t)}{r_{\text{с}}+h_{\text{к}}(1-\exp(-a_4t))}+\ln\frac{\sqrt{2.66\kappa t}}{r_{\text{в}}(t)}\Big) \quad (30)$$

When setting different values $r_{\text{В}}(t_i) > r_c + h_к(1 - e^{-a_4t})$, in the computer program using the method of successive approximations, we can find $r_{\text{В}}(t_i)$ at the time t_i, from (4). It can be also done by using the graph-analytical method, constructing graphs $M_i(r_{\text{В}}(t_i))$ and $N_i(r_{\text{В}}(t_i))$ and determining the point of their interaction, which gives the radius value $r_{\text{В}}(t_i)$ at the time t_i.

Data for calculations: h = 1 m (per 1 m of the thickness of formation); $\mu = \mu_{\text{Ф}} = 1.1\cdot10^{-3}$ Pa·s; $k = 10^{-10}$; 10^{-8}; 10^{-6} m^2 [for sands with various structure filtration factor $k_{\text{Ф}} = k\rho g/\mu$ was estimated by hydroheologists within a range (1.5–1150)$\cdot10^{-6}$ m/s; ρ = 1010 kg/m^3 – water density; g = 9.81 m^2/s – acceleration of gravity]; m = 0.20–0.45; (5–15)$\cdot10^{-3}$ m; $k_{\text{Г}} = 10^{-12}$–10^{-10} m^2; $\beta_c = 2.886\cdot10^{-10}$ Pa^{-1}. The solution is based on two equations (19) and (21) obtained by numerical method. For example, for one moment of time t_{87} (3 days) when i = 87, graphoanalytical definition to illustrate the solution is shown in Figure 5.

The following coefficients were considered: a_1 = 0.000000205; a_2 = 0.47; a_3 = 0.0000205; a_4 = 0.19; a_5 = 0.0045; a_6 = 0.16; a_7 = 1; a_8= 1 – 0.22; 2 – 0.2; 3 – 0.18; 4 – 0.16; 5 – 0.14; 6 – 0.12; 7 – 0.1, i.e. in 3 days displacement zone radius is 20.913 m. Using a computer program we obtain $r_{\text{В}}(t_i)$, using formula (19) we get $Q_i(t)$ at the moment of time t_i and using formula (21) – accumulated flow rate $Q_{Hi}(t_i)$, which is shown in Figure 6.

Using current flow rate $Q_i(t_i)$, we can calculate pressure-loss in each zone – $\Delta p_{\text{Г}}(t_i)$, $\Delta p_{\text{к}}(t_i)$, $\Delta p_{\text{В}}(t_i)$, and then respectively we can obtain shares by total pressure loss value Δp, for each zone i.e. $\varphi_{\text{Г}}(t_i) = \Delta p_{\text{Г}}(t_i)/\Delta p$, $\varphi_{\text{к}}(t_i) = \Delta p_{\text{к}}(t_i)/\Delta p$, $\varphi_{\text{В}}(t_i) = \Delta p_{\text{В}}(t_i)/\Delta p$, $\varphi_{\text{В.З.}}(t_i) = \Delta p_{\text{В.З.}}(t_i)/\Delta p$, according to the results we can build graphs of change $\varphi_{\text{Г}}(t_i)$, $\varphi_{\text{к}}(t_i)$, $\varphi_{\text{В}}(t_i)$, $\varphi_{\text{В.З.}}(t_i)$ for each t_i, i.e. when $i = 0 - n$, where n – number of all intervals of time (to illustrate the colleration, given data are shown in single figure).

Control of accuracy is evaluated by formula:

$$\sum_1^4 \varphi_j(t_i) \approx 1 \quad (31)$$

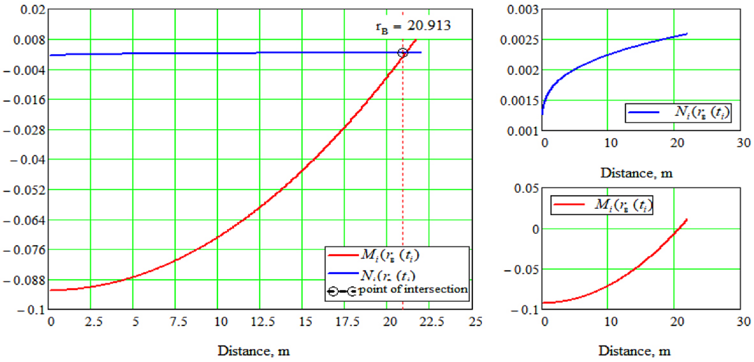

Figure 5. Example of graphoanalytical definition of radius $r_B(t_i)$ at the moment of time equals three days at average permeability conditions

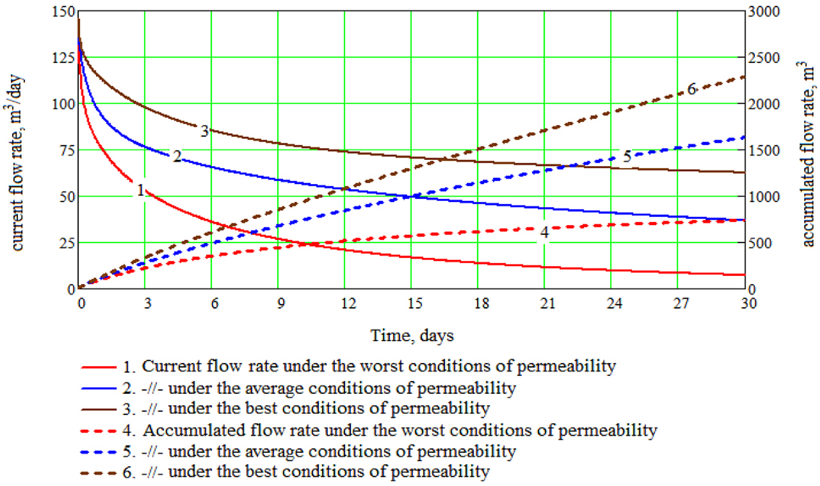

Figure 6. Change of operating flow rate Q_i and accumulated flow rate $Q_н$ during the time t for different conditions of absorption: I best conditions: $a_1 = 0.000025$; $a_2 = 0.1$; $a_3 = 0.22$; $a_4 = 0.0001$; $a_5 = 0.16$; $a_6 = 0.2$; $a_7 = 0.004$; $a_8 = 0.22$; II average conditions: $a_1 = 0.0000205$; $a_2 = 0.16$; $a_3 = 0.16$; $a_4 = 0.0000205$; $a_5 = 0.19$; $a_6 = 0.16$; $a_7 = 0.0045$; $a_8 = 0.16$; III worst conditions: $a_1 = 0.0001$; $a_2 = 0.22$; $a_3 = 0.1$; $a_4 = 0.0000025$; $a_5 = 0,3$; $a_6 = 0.1$; $a_7 = 0.001$; $a_8 = 0.1$.

where: j – number of selected zones ($j = 4$). If this sum does not equal one, Δt rate should be reduced.

Calculations are done using obtained formulas $r_B(t_i)$, $Q_i(t_i)$, $Q_{Hi}(t_i)$, pressure losses in each zone, each zone share by pressure loss, influence of wall cake and wall packing on pressure losses were evaluated, total volume of filtrate in water layer and its percentage of water volume with different densities in oil wells.

Further calculations are performed for the best, average and worst conditions regarding the passage of the filtrate and a combination of the corresponding values of the parameters (k, h_r, Δp) and the empirical coefficients (a_1, a_2, a_3, a_4, a_5, a_6, a_7, a_8), shown in Figure 7.

Analyzing these graphic dependencies, we can state that ratio of pressure losses in displacement of water by filtrate zone and in zone of unsteady filtration of reservoir water to the total given pressure loss $\varphi_B(t_i)$ and $\varphi_{B.3.}(t_i)$ vary quite sharply within time interval from 0 to 3 days and in the future, we observe a smooth decrease in the first case and a smooth increase in the second one. At the same time when the ratio of pressure losses in zone of intraporous colmatation and the zone of filter cake to the total given pressure losses $\varphi_Г(t_i)$ and $\varphi_к(t_i)$ vary within the range from 0 to 0.004 shares of unit, i.e., their influence is less significant. In this case we can see a gradual increase of these dependencies from the first day up to the 30 days (Fig. 8).

Similar conclusions are made by Figure 9 since the nature of graphic dependencies is the same. The difference is in the fact that in this case there are values of coordinates in MPa which

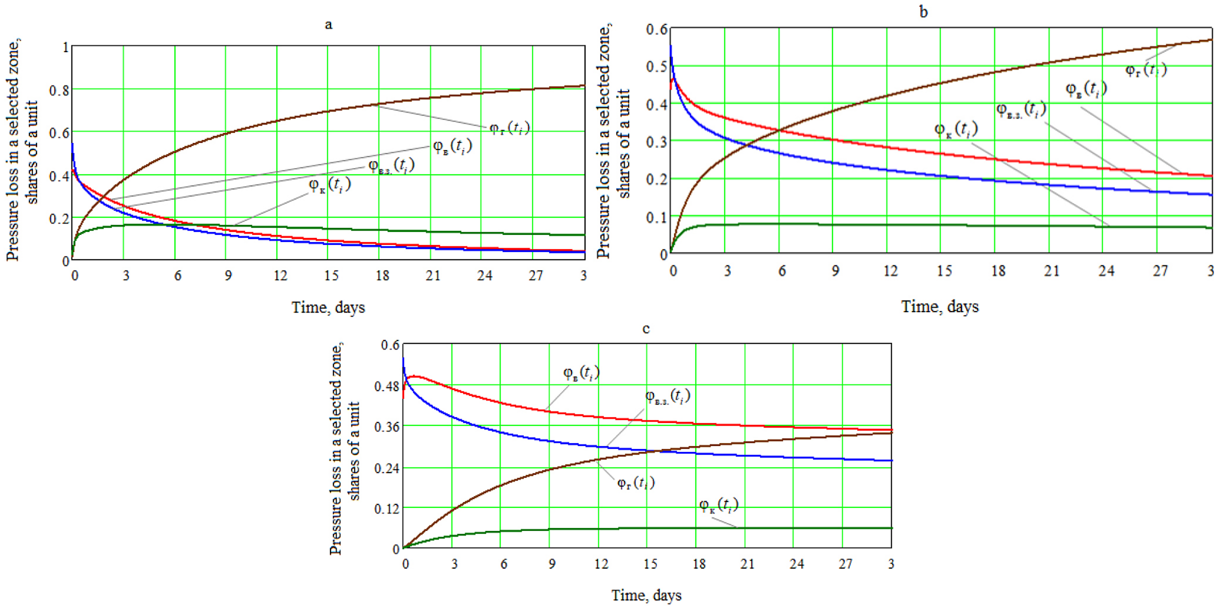

Figure 7. Change in the ratio of pressure losses in each zone to the total given pressure loss $\varphi_Г(t_i)$, over time t_i for the worst (a), average (b) and best (c) penetration conditions: I best conditions: a_1 = 0.000025; a_2 = 0.1; a_3 = 0.22; a_4 = 0.0001; a_5 = 0.16; a_6 = 0.2; a_7 = 0.004; a_8 = 0.22; II average conditions: a_1 = 0.0000205; a_2 = 0.16; a_3 = 0.16; a_4 = 0.0000205; a_5 = 0.19; a_6 = 0.16; a_7 = 0.0045; a_8 = 0.16; III worst conditions: a_1 = 0.0001; a_2 = 0.22; a_3 = 0.1; a_4 = 0.0000025; a_5 = 0,3; a_6 = 0.1; a_7 = 0.001; a_8 = 0.1.

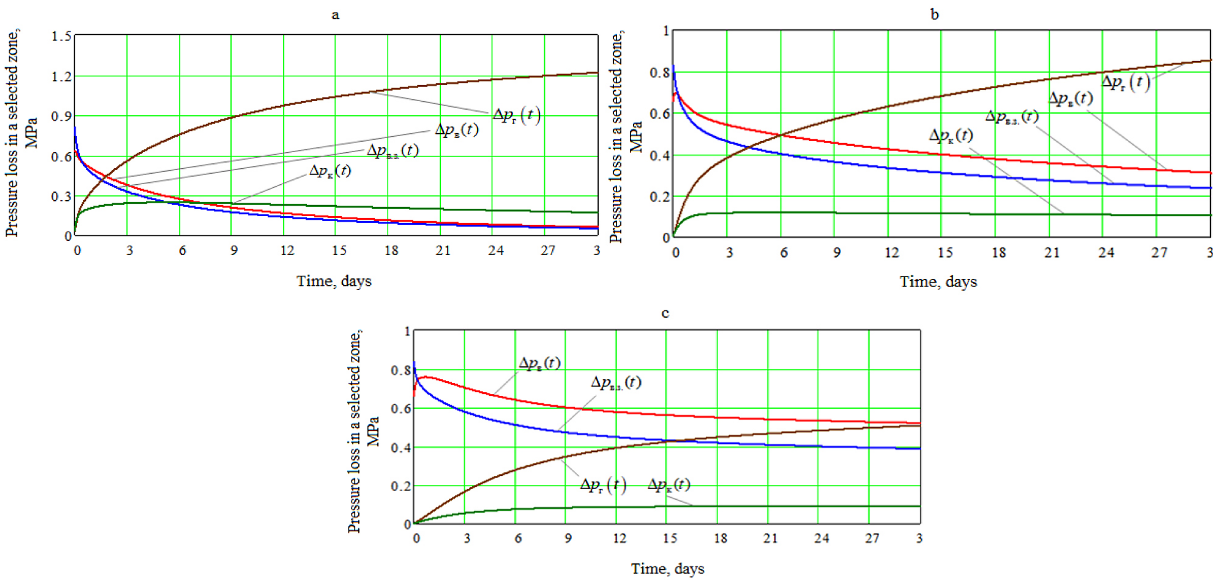

Figure 8. Change of pressure losses in each zone $\Delta p_Г(t)$, $\Delta p_к(t)$, $\Delta p_В(t)$, $\Delta p_{В.З}(t)$ over time t_i for worst (a), average (b) and best (c) conditions of permeability: I best conditions: a_1 = 0.000025; a_2 = 0.1; a_3 = 0.22; a_4 = 0.0001; a_5 = 0.16; a_6 = 0.2; a_7 = 0.004; a_8 = 0.22; II average conditions: a_1 = 0.0000205; a_2 = 0.16; a_3 = 0.16; a_4 = 0.0000205; a_5 = 0.19; a_6 = 0.16; a_7 = 0.0045; a_8 = 0.16; III worst conditions: a_1 = 0.0001; a_2 = 0.22; a_3 = 0.1; a_4 = 0.0000025; a_5 = 0,3; a_6 = 0.1; a_7 = 0.001; a_8 = 0.1

enables to estimate the change of pressure losses in time for each of the four zones in system units.

Change in the radius of permeability of the drilling filtrate over time for three selected cases has a similar nature of gradual increase over the entire period of time, although a sharper change in the graph from the moment of time up to 3 days which equals zero can be distinguished.

Also, total volume of filtrate entering a water layer and its ratio to water volume for selected density of rectangular oil wells were calculated. Following data for calculation was considered:

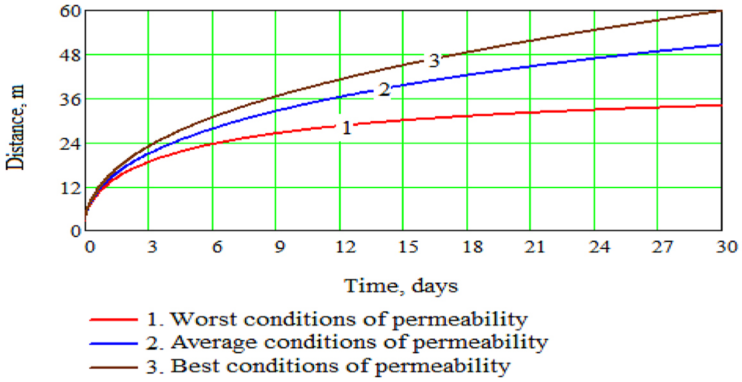

Figure 9. Change of permeability of drilling mud filtrate into the rock formation over time t_i for worst permeability conditions (a), average (b) and best one's (c): I best conditions: $a_1 = 0.000025$; $a_2 = 0.1$; $a_3 = 0.22$; $a_4 = 0.0001$; $a_5 = 0.16$; $a_6 = 0.2$; $a_7 = 0.004$; $a_8 = 0.22$; II average conditions: $a_1 = 0.0000205$; $a_2 = 0.16$; $a_3 = 0.16$; $a_4 = 0.0000205$; $a_5 = 0.19$; $a_6 = 0.16$; $a_7 = 0.0045$; $a_8 = 0.16$; III worst conditions: $a_1 = 0.0001$; $a_2 = 0.22$; $a_3 = 0.1$; $a_4 = 0.0000025$; $a_5 = 0,3$; $a_6 = 0.1$; $a_7 = 0.001$; $a_8 = 0.1$.

distance between the wells 2σ = 200 m, the thickness of the layer h = 1 m, radius of penetration zone for filtrate in aqueous layer r_w = 59.47 m, time of penetration t = 30 days. The amount of filtrate penetrating into the formation (for average conditions) during the calculated time is 2267 m^3 and percentage will be equal to 8.123%. Such a result will be obtained for one well only. As the number of drilled wells grows, the amount of mud penetrated in aqueous layer well increase proportionally. It should also be taken into account that the contaminated water will be mixed with the pure water and thus the radius of filtrate penetration will increase even more.

CONCLUSION

The hydrodynamic interaction of an open oil or gas wellbore during their drilling near the fresh water formation was investigated for the first time. Four zones (clay crust, intraporous colmatation, water displacement by filtrate, unstable perturbation of pressure) are distinguished according to the filtration characteristics, and the mathematical model of the invasion process is created. The influence of each zone on the amount of pressure drop was determined, as well as the change in the filtrate flow and accumulated flow in time were determined under three conditions of invasion. It was pointed out that the clay crust zones and intraporous colmatation are dominant, so it may be feasible to assure the quality of the mud in relation to the capacity of the colmatation or other technological and technical tools. The amount of filtrate invaded into the water formation can significantly reduce the quality of fresh water and cause environmental damage.

Acknowledgements

Special thanks to Professor Vasyl Boyko, without whose wise advice this study would not be of such quality.

This study was supported by the National research fund of Ukraine.

REFERENCES

1. Gleeson, T., Alley, W.M., Allen, D.M., Sophocleous, M.A., Zhou, Y., Taniguchi, M., VanderSteen, J. 2012. Towards sustainable groundwater use: Setting long-term goals, backcasting, and managing adaptively. Groundwater, 50(1), 19-26.
2. Chi, G. and Xue, C. 2011. An overview of hydrodynamic studies of mineralization. Geoscience Frontiers, 2(3), 423-438.
3. Tikhomirov, V.V. 2018. Hydrogeochemistry Fundamentals and Advances, Environmental Analysis of Groundwater, Vol. 3. John Wiley & Sons.
4. Adamenko, Y.S., Arkhypova, L.M., Mandryk, O.M. 2017. Territorial normative of quality of hydroecosystems of protected territories. Hydrobiological Journal, 53(2), 50-58. doi:10.1615/HydrobJ.v53.i2.50
5. Shokri-Kuehni, S.M., Rad, M.N., Webb, C., Shokri, N. 2017. Impact of type of salt and ambient conditions on saline water evaporation from porous media. Advances in water resources, 105, 154-161.
6. Misch, D., Gross, D., Mahlstedt, N., Makogon, V., Sachsenhofer, R.F. 2016. Shale gas/shale oil

potential of upper Visean Black Shales in the Dniepr-Donets Basin (Ukraine). Marine and Petroleum Geology, 75, 203-219.

7. Sephton, M.A. and Hazen, R.M. 2013. On the origins of deep hydrocarbons. Reviews in Mineralogy and Geochemistry, 75(1), 449-465.
8. Maievskyi B.Y. 2014. Aktualni problemy naftohazovoi heolohii. Ivano-Frankivsk: IFNTUNG [in Ukrainian].
9. Boiko V.S., Mandryk O.M., Zeljmanovych A.I. 2017. Peretikannja pidzemnykh vod mizh plastamy i struktury potokiv, jakistj zmishanykh vod i ekologhichnyj zakhyst. Ekologhichna bezpeka ta zbalansovane resursokorystuvannja. Ivano-Frankivsjk, 2(16), 28-43.
10. Mandryk, O., Pukish, A., Zelmanovych, A. 2017. Formation peculiarities of physical and chemical composition of highly mineralized edge water. Mining of Mineral Deposits, 11(1), 72–79.
11. World Health Organization, 2016. Protecting surface water for health: identifying, assessing and managing drinking-water quality risks in surface-water catchments.
12. Reddy, C.M., Arey, J.S., Seewald, J.S., Sylva, S.P., Lemkau, K.L., Nelson, R.K., ... Camilli, R. 2012. Composition and fate of gas and oil released to the water column during the Deepwater Horizon oil spill. Proceedings of the National Academy of Sciences, 109(50), 20229-20234.
13. ASME Shale Shaker Committee, 2011. Drilling fluids processing handbook. Elsevier.
14. Mysliuk M.A. 2002. Burinnja sverdlovyn: Dovidnyk. U 5t. Kyjiv: “Interpres LTD” [in Ukrainian].
15. Veil, J.A. 2002. Drilling waste management: past, present, and future. In: SPE annual technical conference and exhibition. Society of Petroleum Engineers.
16. Bakke, T., Klungsøyr, J., Sanni, S. 2013. Environmental impacts of produced water and drilling waste discharges from the Norwegian offshore petroleum industry. Marine Environmental Research, 92, 154-169.
17. Chudyk, I., Poberezhny, L., Hrysanchuk, A., & Poberezhna, L. 2019. Corrosion of drill pipes in high mineralized produced waters. Procedia Structural Integrity, 16, 260-264.
18. Mandryk, O.M., Arkhypova, L.M., Pukish, A.V., Zelmanovych, A., Yakovlyuk, K. 2017. Theoretical and methodological foundations of sustainable development of Geosystems. In: IOP Conference Series: Materials Science and Engineering, 200(1), art. no. 012018. IOP Publishing.
19. Pietrzak, D., Mandryk, O., Wątor, K., Kmiecik, E., & Zelmanowych, A. 2018. Evaluation of the possibility of using the water of the Bystrytsya-Nadvirnyans’ka River in Cherniiv (Ukraine) to supply the population with drinking water. In: E3S Web of Conferences, 30, art. no. 01009. EDP Sciences.
20. Thomas, S. 2008. Enhanced oil recovery-an overview. Oil & Gas Science and Technology-Revue de l’IFP, 63(1), 9-19.
21. Barlow, P.M. 2003. Ground water in freshwater-saltwater environments of the Atlantic coast. Geological Survey, 1262.
22. Huang, C., Zheng, X.L., Luan, X.M., & Li, Y.X. 2009. Experimental study of changes in hydraulic conductivity of aquifer medium in salt-freshwater displacement process. Hydrogeology & Engineering Geology, 36(6), 21-25.
23. Reilly, T.E., & Goodman, A.S. 1985. Quantitative analysis of saltwater-freshwater relationships in groundwater systems – a historical perspective. Journal of Hydrology, 80(1-2), 125-160.
24. Christiansen, I.P. 1973. Numerical simulation of hydrodynamics by the method of point vortices. Journal of Computational Physics, 13(3), 363-379.
25. Boiko V.S., Mishchuk B.M. Probabilistic behavior of well rate decrease laws through time. Universal dependence of Weibull-Makeham law // Journal of hydrocarbon power engineering. – Ivano-Frankivsk: IFNTUOG, 2014. - №1(1). -P. 5 – 12.
26. Caenn, R. and Chillingar, G.V. 1996. Drilling fluids: State of the art. Journal of Petroleum Science and Engineering, 14(3-4), 221-230.
27. Mitchell, R.F., Ravi, K., Pgs, H. 2006. Drilling Engineering. In: Lake, L.W. (Ed.) Petroleum Engineering Handbook, Society of Petroleum Engineers: Richardson, TX.
28. Ghassal, Bandar I. Reservoir connectivity, water washing and oil to oil correlation: An integrated geochemical & petroleum engineering approach. SPE Middle East Oil and Gas Show and Conference, Manama, Bahrain, March 2019. https://doi.org/10.2118/194957-MS.
29. Goldberg, V.M. 1976. Hydrogeological forecasts of ground – water quality in water intake areas.